Compression of X-ray Free Electron Laser Pulses to Attosecond Duration

James Sadler,[1] Raoul Trines,[2] Robert Bingham,[2,3] Luke Ceurvorst,[1] Naren Ratan,[1]
Muhammad Firmansyah Kasim,[1] Ricky Nathvani,[1] Piotr Oleśkiewicz,[1] and Peter Norreys[1,2]

[1] *Clarendon Laboratory, University of Oxford, Parks Road, Oxford OX1 3PU*
[2] *Central Laser Facility, STFC Rutherford Appleton Laboratory, Didcot, Oxon, OX11 0QX*
[3] *Department of Physics, University of Strathclyde, John Anderson Building, 107 Rottenrow, Glasgow, G4 0NG*

(Dated: March 13, 2015)

State of the art X-ray Free Electron Laser facilities currently provide the brightest X-ray pulses readily available, typically with mJ energy and several hundred femtosecond duration. Here we present one- and two-dimensional Particle-in-Cell simulations, utilising the process of stimulated Raman amplification, showing that these pulses are compressed to a temporally coherent, sub-femtosecond pulse at 8% efficiency. One or more sequential pulses of this type may pave the way for novel attosecond scattering experiments, probing the evolution of bound electron wavefunctions. Furthermore, evidence is presented that significant Landau damping and wavebreaking may be beneficial in distorting the rear of the interaction and further reducing the final pulse duration.

In recent years, outputs from facility scale X-ray Free Electron Lasers (XFELs) have set new boundaries for the brightest X-ray sources available, improving on synchrotron sources by at least nine orders of magnitude. Current facilities such as the Stanford Linac Coherent Light Source (LCLS) [1] are greatly over subscribed and many new facilities are in development, such as the European XFEL [2] in the DESY Laboratory in Germany and the the SACLA facility in Japan. The pulses generated by these machines have contributed to research areas as diverse as protein crystallography [3], phase transitions [4] and superconductors [5].

The XFEL wavelength is variable from soft X-rays down to the angström level and the power output consists of a stochastic series of intensity spikes. Recent advances in seeding the emission process and use of a low bunch charge will lead to a reduction in pulse duration to a few femtoseconds [6, 7]. Despite this improvement in pulse quality, more work needs to be done to reduce the pulse duration further, as even a few femtosecond output still exceeds the timescale of atomic bound electron processes [8]. Energetic attosecond pulses are also desirable for better resolution in destructive scattering experiments where the timescale of molecular destruction in an intense X-ray beam is of the order 1 fs [9]. Although attosecond pulses can be generated via interference with high harmonics [10], previous experiments report the need for sub-femtosecond pulses with greater fluence [11]. This paper reports the first comprehensive computational study of pulse compression (associated with amplification via stimulated Raman backward scattering (RBS) in an underdense plasma) to transfer some of the energy of a typical XFEL pulse to a much shorter, but still highly energetic sub-femtosecond pulse.

Extensive analytical [12–14] and computational studies [15] of Raman amplification in the optical regime have shown that a pump laser pulse may transfer its energy to a much shorter counter-propagating seed pulse, finishing at up to 1000 times the pump pulse power. Simulations at infrared wavelengths have shown efficiencies of 30% or more, leaving output pulses in the petawatt regime [16]. Experiments on Gigawatt infra-red (IR) pulses [17] have shown that as the seed grows to greater intensity than its pump, the energy transfer continues towards the seed pulse.

Beneficial Raman backscattering can be stimulated by the counter-propagation of a pump pulse at frequency ω_0 and a seed pulse at frequency $\omega_0 - \omega_p$ (where ω_p is the electron plasma frequency) and around 1/1000th the duration. The region where they overlap is an underdense plasma with electron density n_e around 1% of the critical density n_{crit}. This means both pulses propagate almost as if in vacuum. The beating of these pulses resonantly excites an electron plasma (Langmuir) wave at frequency ω_p and approximate wavenumber $2\omega_0/c$ for very underdense plasmas. The pump pulse then couples with this density perturbation and the lower Stokes compo-

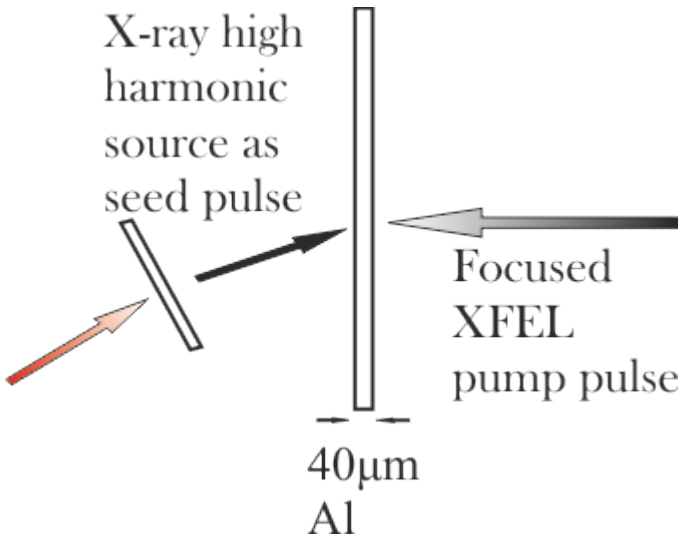

FIG. 1. A schematic of the proposed experimental setup. Pump pulse has wavelength $1 - 10$ nm and energy 3 mJ or above.

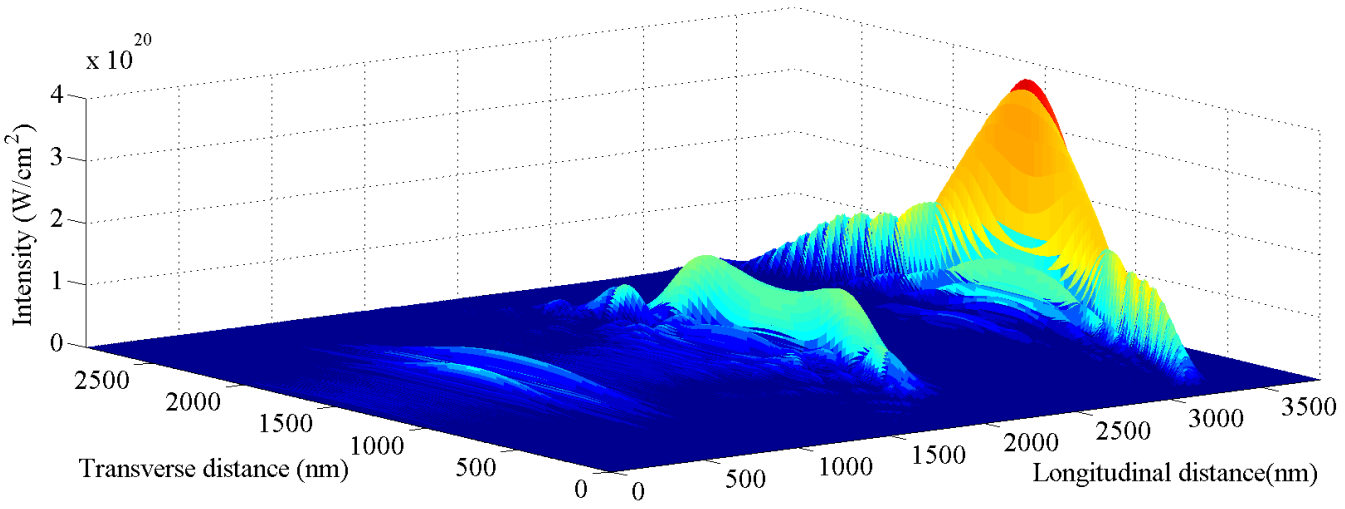

FIG. 2. A two-dimensional Particle-in-Cell simulation of the X-ray seed intensity as it propagates to the right, through the pump pulse (almost invisible on this scale) in the opposite direction. Time steps are after 16%, 70% and 100% of the interaction distance. Parameters are mid-range of the window used in FIG.I. Computational restraints meant only one-dimensional simulations included collisions and so this figure may only be taken as indicative. Distance between successive time steps is not to scale.

nent amplifies the seed, leading to a parametric instability with growth rate $\gamma \propto I_0^{\frac{1}{2}} n_e^{\frac{1}{4}} \lambda_0^{\frac{1}{2}}$, where I_0 and λ_0 are the pump intensity and wavelength respectively.

The theory of this instability is scale invariant provided that $I_0\lambda_0^2$, n_e/n_{crit} and the ratio of the pump to seed pulse duration are kept fixed. Therefore as noted in reference [18], their optimal results may be equally applicable to a 10 nm soft X-ray pump pulse. The required scaled pump intensity is $5 \times 10^{18}\,\mathrm{W/cm^2}$ and electron density 5×10^{22} cm^{-3} (less than 1% of critical density). These are parameters directly accessible to an X-ray free electron laser focused to a spot size of 1-2 μm, a feat achieved at shorter wavelengths by a group at the SACLA laser in Japan [19]. A typical pulse duration of 250 fs means the target is a 40 μm solid density foil.

One may use this scale invariance to assess the optimal pump pulse wavelength. Keeping ω_p/ω_0 fixed while scaling all distances linearly, the number of e-foldings is $\gamma L/c \propto P_0^{\frac{1}{2}}\lambda_0/D$ where P_0 is the peak power, D is the spot size and L is the interaction distance. Both the XFEL pulse power [20] and the ratio λ/D will decrease as we go to harder X-rays. Therefore high power long wavelength pump pulses of $\lambda = 10$ nm were considered.

However, one must be careful in using the scale invariance to extrapolate the results of previous studies at optical wavelengths into this regime. Gas jet experiments at optical wavelengths generate a classical collisionless plasma at a density four orders of magnitude lower than the soft X-ray case considered here. In this case, both Landau damping and collisional damping will be much more pronounced than those studies at optical/IR wavelengths. This can be seen by estimating the ratio of the Langmuir wave phase velocity to a typical thermal velocity and calculating the plasma parameter:

$$\frac{v_p}{v_{th}} = \frac{\omega_p}{2\omega_o}\sqrt{\frac{m_e c^2}{K_B T_e}} \simeq 11\frac{\omega_p}{\omega_0}T_e^{-\frac{1}{2}} \tag{1}$$

$$n_e\lambda_D^3 \simeq 1.3 \times 10^{13} n_e^{-\frac{1}{2}} T_e^{\frac{3}{2}} \tag{2}$$

With electron density in units of cm^{-3} and electron temperature in units of keV. All other symbols have their usual meanings.

The one-dimensional (1D) radiation hydrodynamic code Helios [21] was initially used to estimate conditions in the plasma under irradiation by the focused pump pulse. A 40 μm plastic (CH) plasma slab with density 5×10^{22} cm^{-3} and Spitzer resistivity was modelled with a 200 eV starting temperature. For a typical 100 fs irradiation at intensity $10^{18}\,\mathrm{W/cm^2}$, almost uniform electron temperatures of 400 eV are predicted in the dense target plasma once the pump radiation had passed through. This leads to a value of 1.3 for (1) and a Maxwellian averaged Landau damping rate of $\Gamma \simeq 0.3\omega_p$. Collisions are also important on the timescale ω_p^{-1} as the value of $n_e\lambda_D^3$ is 14-20. One therefore concludes that the plasma is fairly collisional and Landau dominated.

As predicted by Malkin *et al.* [18] there is a cut-off wavelength below which Raman amplification becomes unfeasible due to heavy collisional damping of the pump pulse and/or heavy Landau damping suppressing the plasma wave. In order to minimise these damping rates, opposite conditions are needed and so some damping of the wave has to be accepted. From Malkin *et al.*'s analytical results, the cut-off is in the region of 1 nm for these

Pump Intensity (x 10^{18} W/cm^2)	Electron Density (n/n_{crit})							
	0.30%		0.51%		0.69%		1.0%	
1.4			5.6	1400	9.5	1280		
			0.04	1.1%	0.06	1.7%		
5.5			620	370	240	400	400	480
			1.1	8.0%	0.4	3.5%	1.0	7.0%
12.3	450	330	800	290	880	260		
	0.7	2.4%	1.2	3.8%	1.1	3.7%		

TABLE I. Results for 1D PIC simulations with a pump wavelength of 10 nm and fixed duration 250 fs. For a variety of pump intensities and plasma electron densities, the following output pulse parameters are given: Peak intensity ($\times 10^{18}$ W/cm^2, blue), duration (as, green), energy content assuming 1um spot size (mJ, pink) and energy transfer efficiency (orange). Density is given in proportion to the critical plasma density.

parameters. Even above this threshold, the efficiency will be lowered by these damping processes [22]. This was another reason to investigate longer wavelengths first.

The RBS process has a non-linear super-radiant regime [23]. However, even with optimistic parameters [20] from the forthcoming European XFEL facility the seed will not become intense enough to enter this regime. This was verified in our simulations, that is to say that the process remains in the linear regime where pump depletion is small and intensity growth of the seed pulse is exponential. This is another contributing factor to the low efficiency at X-ray wavelengths.

Of course, other growing instabilities are also present and the relative growth rates of these compared to Raman backscatter will affect the performance of the amplifier. Lead among these are Raman forward scatter, producing longitudinal modulations to the pulse, and filamentation, producing a transverse breakup. These effects are a hindrance but there exists an optimal parameter window where the e-foldings of these unwanted instabilities are minimised while still giving effective amplification. The focused intensities exceed the filamentation threshold set by Bingham *et al.* [24] However their characteristic growth distance of the thermal filamentation for soft X-rays reduces to

$$\frac{\lambda_{fil}}{\lambda_0} = 8\frac{\omega_0^2}{\omega_p^2}\frac{v_{th}^2}{a_0^2 c^2}.$$

With V_{th} the electron thermal velocity and a_0 the dimensionless vector potential, having the range 0.01-0.03 for these parameters. This suggests $\lambda_{fil} > 1000\lambda_0$, showing the interaction is over before heavy thermal filamentation sets in. In any case, thermal filamentation is of less concern for this experiment as the seed will not be subsequently focused as for proposed schemes with optical pulses. The energy transfer efficiency and final pulse duration are the more important factors to optimise. In addition, Raman forward scatter is minimised for $n_e/n_{crit} < 0.01$.

These considerations indicate an optimal parameter window of $\lambda = 1 - 10$ nm, with a range of intensities and plasma densities shown in the results Table I. This window was explored with 1D simulations performed using the Particle-in-Cell (PIC) code Osiris [25]. A fixed simulation window of width 45 μm contained a uniform plasma of width 40 μm. This was divided into 120 cells per wavelength and 50 electrons per cell, in order to fully model any thermal effects. A flat pump pulse of wavelength 10 nm and duration 250 fs counter-propagates with a Gaussian seed pulse of initial duration 1.5 fs Full Width at Half Maximum (FWHM) and peak intensity equal to the pump intensity. Its wavelength was calculated via the frequency matching condition including the Bohm-Gross correction [26]:

$$\omega \simeq \omega_0 - \omega_p\sqrt{1 + 12\left(\frac{\omega_0}{\omega_p}\right)^2\frac{K_B T_e}{m_e c^2}}$$

where a very underdense plasma is assumed.

Due to the collisional nature of the plasma, 1D simulations included a routine to model the electron-ion and electron-electron collisions, where relativistic effects are accounted for. The initial plasma temperature was 200 eV, with collisional damping causing a rise to around 500 eV after the pump has propagated through the plasma, in agreement with the 1D hydrodynamic simulations.

Table I shows the results of these 1D simulations. Currently the highest pump pulse intensities available are limited to the top row of Table I, however one can see the performance dramatically increases for higher intensities due to the increased linear RBS growth rate. The European XFEL beam may reach intensities towards the bottom of Table I. Better focusing of the X-ray pulses, or future upgrades, will allow pulses to be compressed down to a few hundred attoseconds and still retain up to 8% of the pump energy. Notice that the performance is generally seen to increase with higher densities. However, it is best to keep to less than 0.6% of critical density to reduce the growth of competing plasma instabilities. Smoother pulse envelopes and lower prepulses (by a factor of 100) were observed for the simulations at lower plasma density.

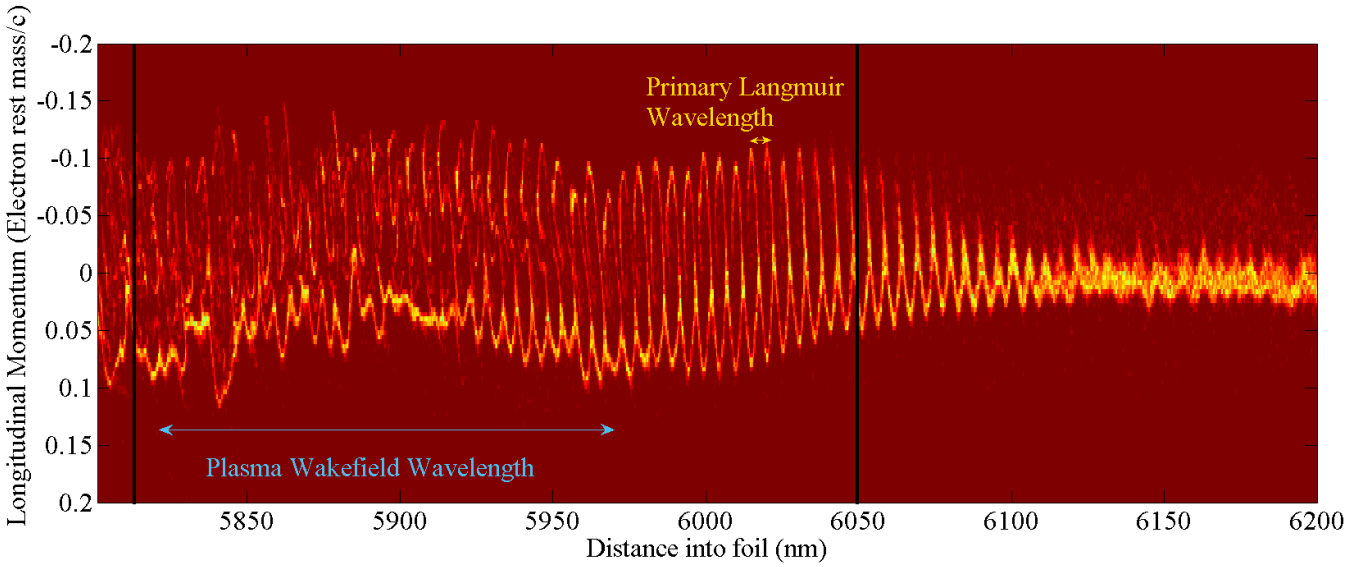

FIG. 3. Electron phase space diagram for a 1D PIC simulation after 15% of the interaction distance. The FWHM of the seed pulse is enclosed by the solid black lines. The initial Maxwellian distribution is excited to a Langmuir wave which subsequently breaks within the extent of the seed pulse.

The intensities here are slightly above the plasma wave breaking threshold [27, 28]:

$$I_{thresh} = \frac{1.7 \times 10^{23}}{\lambda_0^2} \left(\frac{\omega_p}{\omega_0}\right)^3$$

With the pump wavelength in units of nm and intensity in $\mathrm{W/cm^2}$. To investigate the compressional effects of wave-breaking, further 1D simulations were undertaken. These had similar parameters to Table I. In the case where the initial seed intensity was ten times the pump intensity, the electron phase space diagram, shown in FIG. 3, is plotted near the start of the interaction. The perturbation with wavelength 150 nm (equal to the plasma wavelength) corresponds to a wakefield excited by the seed pulse. This damps away and dissipates energy from the seed. The short wavelength Langmuir wave is excited right from the front of the seed pulse but only manages around 20 periods of oscillation before it breaks. This places an upper limit on the final duration of the seed. In addition, the distribution is skewed towards negative momentum, suggesting heavy Landau damping from the plasma wave travelling at $-0.03c$. This rests in agreement with the estimate given by equation (1). From the position of the seed pulse FWHM, one can see that both of these effects will cease amplification near the back of the seed pulse and help to shorten it, as the front is amplified more than the rear.

In a further simulation scaled for a wavelength of 1 nm at constant $I_0\lambda_0^2$, the efficiency was comparable to the 10 nm case. However a typical XFEL pulse has lower power at shorter wavelengths. A second simulation with realistic parameters showed lower coupling to the seed (by a factor of 10) but still produced coherent sub-femtosecond radiation.

Previous proposals for attosecond pulse generation have centred on manipulating electron bunches. The results of this study indicate another feasible route through utilising the immense X-ray intensity of XFELs in combination with laser-plasma interactions. Experiments with relativistic plasma irradiation by infrared pulses have already yielded high harmonics into the X-ray band [29–32], giving a promising candidate for such a seed pulse. The broad spatial extent of these harmonics will ease requirements for precision alignment. In addition, the high repetition frequency of harmonic radiation eases the required temporal synchronisation with the XFEL pulse in single shot mode. In this way, over $0.1\,mJ$ of XFEL energy may be compressed into a 200 as, 6 cycle soft X-ray laser pulse.

We also note that the scheme proposed here causes only minor depletion of the pump pulse and so a train of harmonics may propagate through the pump one after the other and be amplified to nearly the same level. This could provide a train of isolated attosecond pulses, with controllable spacing defined by the details of the high harmonic generation. Radiation of this sort would open new frontiers in attosecond science and the study of ultrafast processes.

ACKNOWLEDGMENTS

The authors would like to thank the Central Laser Facility computer science staff and the Osiris consortium. This research was funded by EPSRC grant number EP/L000237/1. Simulations were performed with resources on the STFC Scarf cluster and the Archer supercomputer facility.

[1] J. Arthur, G. Materlik, R. Tatchyn, and H. Winick, Review of scientific instruments **66**, 1987 (1995).

[2] M. Altarelli, R. Brinkmann, M. Chergui, W. Decking, B. Dobson, S. Düsterer, G. Grübel, W. Graeff, H. Graafsma, J. Hajdu, *et al.*, Technical Design Report, DESY **97**, 2006 (2006).

[3] S. Boutet, L. Lomb, G. J. Williams, T. R. Barends, A. Aquila, R. B. Doak, U. Weierstall, D. P. DePonte, J. Steinbrener, R. L. Shoeman, *et al.*, Science **337**, 362 (2012).

[4] S. P. Hau-Riege, A. Graf, T. Döppner, R. A. London, J. Krzywinski, C. Fortmann, S. Glenzer, M. Frank, K. Sokolowski-Tinten, M. Messerschmidt, *et al.*, Physical review letters **108**, 217402 (2012).

[5] M. Först, R. Tobey, H. Bromberger, S. Wilkins, V. Khanna, A. Caviglia, Y.-D. Chuang, W. Lee, W. Schlotter, J. Turner, *et al.*, Physical review letters **112**, 157002 (2014).

[6] J. Amann, W. Berg, V. Blank, F.-J. Decker, Y. Ding, P. Emma, Y. Feng, J. Frisch, D. Fritz, J. Hastings, *et al.*, Nature photonics **6**, 693 (2012).

[7] P. Emma, R. Akre, J. Arthur, R. Bionta, C. Bostedt, J. Bozek, A. Brachmann, P. Bucksbaum, R. Coffee, F.-J. Decker, *et al.*, nature photonics **4**, 641 (2010).

[8] F. Krausz and M. Ivanov, Reviews of Modern Physics **81**, 163 (2009).

[9] R. Neutze, R. Wouts, D. van der Spoel, E. Weckert, and J. Hajdu, Nature **406**, 752 (2000).

[10] P. . M. Paul, E. Toma, P. Breger, G. Mullot, F. Augé, P. Balcou, H. Muller, and P. Agostini, Science **292**, 1689 (2001).

[11] M. Hentschel, R. Kienberger, C. Spielmann, G. A. Reider, N. Milosevic, T. Brabec, P. Corkum, U. Heinzmann, M. Drescher, and F. Krausz, Nature **414**, 509 (2001).

[12] V. Malkin, G. Shvets, and N. Fisch, Physical review letters **84**, 1208 (2000).

[13] V. Malkin, G. Shvets, and N. Fisch, Physics of Plasmas (1994-present) **7**, 2232 (2000).

[14] V. Malkin, G. Shvets, and N. Fisch, Physical review letters **82**, 4448 (1999).

[15] R. Trines, F. Fiuza, R. Bingham, R. Fonseca, L. Silva, R. Cairns, and P. Norreys, Physical review letters **107**, 105002 (2011).

[16] R. Trines, F. Fiuza, R. Bingham, R. Fonseca, L. Silva, R. Cairns, and P. Norreys, Nature Physics **7**, 87 (2011).

[17] J. Ren, W. Cheng, S. Li, and S. Suckewer, Nature Physics **3**, 732 (2007).

[18] V. Malkin, N. Fisch, and J. Wurtele, Physical Review E **75**, 026404 (2007).

[19] H. Yumoto, H. Mimura, T. Koyama, S. Matsuyama, K. Tono, T. Togashi, Y. Inubushi, T. Sato, T. Tanaka, T. Kimura, *et al.*, Nature Photonics **7**, 43 (2013).

[20] J. Grünert *et al.*, Proceedings of FEL2009, Liverpool, UK, MPOC56 (2009).

[21] J. MacFarlane, I. Golovkin, and P. Woodruff, Journal of Quantitative Spectroscopy and Radiative Transfer **99**, 381 (2006).

[22] N. A. Yampolsky and N. J. Fisch, Physics of Plasmas (1994-present) **18**, 056711 (2011).

[23] G. Shvets, N. Fisch, A. Pukhov, and J. Meyer-ter Vehn, Physical review letters **81**, 4879 (1998).

[24] R. Bingham, R. Short, E. Williams, D. Villeneuve, and M. Richardson, Plasma physics and controlled fusion **26**, 1077 (1984).

[25] R. A. Fonseca, L. O. Silva, F. S. Tsung, V. K. Decyk, W. Lu, C. Ren, W. B. Mori, S. Deng, S. Lee, T. Katsouleas, *et al.*, in *Computational ScienceICCS 2002* (Springer, 2002) pp. 342–351.

[26] D. Bohm and E. P. Gross, Physical Review **75**, 1851 (1949).

[27] J. M. Dawson, Physical Review **113**, 383 (1959).

[28] A. Bergmann and P. Mulser, Physical Review E **47**, 3585 (1993).

[29] S. Gordienko, A. Pukhov, O. Shorokhov, and T. Baeva, Physical review letters **94**, 103903 (2005).

[30] M. Drescher, M. Hentschel, R. Kienberger, G. Tempea, C. Spielmann, G. A. Reider, P. B. Corkum, and F. Krausz, Science **291**, 1923 (2001).

[31] P. Norreys, M. Zepf, S. Moustaizis, A. Fews, J. Zhang, P. Lee, M. Bakarezos, C. Danson, A. Dyson, P. Gibbon, *et al.*, Physical review letters **76**, 1832 (1996).

[32] B. Dromey, S. Cousens, S. Rykovanov, M. Yeung, D. Jung, D. Gautier, T. Dzelzainis, D. Kiefer, S. Palaniyppan, R. Shah, *et al.*, New Journal of Physics **15**, 015025 (2013).